Joint Multicast Beamforming and Relay Design for Maritime Communication Systems

Ruiyang Duan, *Student Member, IEEE*, Jingjing Wang, *Student Member, IEEE*,

Hongming Zhang, *Member, IEEE*, Yong Ren, *Senior Member, IEEE* and

Lajos Hanzo, *Fellow, IEEE*

Abstract

With growing human maritime activities, supporting low-cost and high-speed information services for users at sea has become imperative. However, traditional means of maritime communications fail to provide high rate services due to their high cost and limited bandwidth. In this paper, considering a base station ashore and several offshore relay nodes, we propose a cooperative multicast communication scheme for maritime users relying on joint beamforming (BF) optimization and relay design. Specifically, we decompose our proposed joint optimization problem into two subproblems, which can be solved by the feasible point pursuit successive convex approximation approach. Furthermore, an alternating optimization algorithm is proposed, which imposes an exponentially increasing complexity as a function of the number of BF elements and the number of relays, when aiming for finding the globally optimal solution. In order to reduce this excessive computational complexity, a low-complexity distributed algorithm is also conceived and its closed-form solution is derived. Finally, the simulation results provided show that our proposed algorithm is beneficial in terms of increasing both the throughput as well as the energy efficiency.

Index Terms

Maritime communications, energy efficiency, multicast beamforming, relay design.

R. Duan, J. Wang and Y. Ren are with the Department of Electronic Engineering, Tsinghua University, Beijing, 100084, China. E-mail: duanry16@mails.tsinghua.edu.cn, chinaeephd@gmail.com, reny@tsinghua.edu.cn.

H. Zhang is with Electrical Engineering Department, Columbia University, New York City, 10027, USA. E-mail: hz2535@columbia.edu.

L. Hanzo is with the School of Electronics and Computer Science, University of Southampton, Southampton, SO17, IBJ, UK. Email: lh@ecs.soton.ac.uk.

I. INTRODUCTION

With the rapid development of the so-called "blue economy", more attention has been focused on a range of ocean-related activities, such as fishery, marine environmental monitoring, offshore exploration, etc. Furthermore, ships have become an important means of transportation both for humans as well as for global trade. In order to guarantee the navigational safety of ships and to provide infotainment services, there is a soaring demand for providing low-cost yet reliable links for multimedia signals. Therefore, numerous initiatives have been launched to pave the way for constructing high rate maritime communication systems [1]–[3].

The existing maritime communication systems typically rely on satellite communications and on very-high-frequency (VHF) communications [4]. For example, satellite communication systems, such as the international maritime satellite system (INMARSAT) [5] and the Iridium system [6], have been developed for providing high rate maritime information services relying on very small aperture terminals (VSAT). However, the corresponding communication cost is prohibitively high. By contrast, the VHF aided legacy maritime communication system cannot support high data-rate multimedia services because of its limited bandwidth. Therefore, it is of utmost importance to develop new techniques for supporting low-cost, high rate multimedia information services.

On the other hand, relay-aided communications have the advantage of extending the coverage area and improving the spatial diversity gain of cooperative wireless networks. As a benefit, they have been widely used in terrestrial broadband communication systems, such as the long-term evolution (LTE) and the worldwide interoperability for microwave access (WiMAX) systems [7]. Recently, relay communication techniques have also been extended to oceanic scenarios for supporting efficient and reliable information services [8]–[10]. In [8], relying on ships and buoys acting as relay nodes (RNs), Zhou *et al*. constructed a multi-hop ship-to-shore wireless mesh network, which attains a coverage of 30 km at 6 Mbps. The video transmission scheduling problem in a 'throw-box' connected maritime delay-tolerant network (DTN) was investigated in [9], where Yang *et al*. proposed a beneficial resource allocation technique for maritime communication systems. Furthermore, for the sake of further improving the system's capacity, multiple antenna techniques were introduced for maritime communication systems in [11]–[14]. Specifically, the comparison of system performance using different antenna

configurations and transmission modes in a centralized maritime multiple-input multiple-output (MIMO) LTE network was investigated by Mroueh *et al.* in [11], showing that as expected, a MIMO system exhibiting the maximum attainable diversity gain outperforms its single-input single-output (SISO) counterpart in long-range maritime communications. In [14], Wei *et al.* proposed a joint vessel-position and transmit power optimization scheme to mitigate the pilot contamination problem in the costal multi-cell multi-user MIMO systems when the associated pilots are not orthogonal to each other. Moreover, benefits of the fog computing and of a large number of distributed antennas (DAs) were quantified in the context of maritime communication systems by Yang *et al.* and Xu *et al.* in [15] and [16], respectively.

As a further development, physical layer multicast beamforming has been recognized as an efficient technique of supporting multimedia broadcast services to users of common interest. In the literature, the multicast beamforming design for a single group of users was modeled as a classical max-min problem by Sidiropoulos *et al.* [17]. A similar problem considering beamforming design for multiple groups was studied in [18]. Furthermore, in [19], Xiang *et al.* proposed a coordinated multicast beamforming algorithm for multi-cell networks by taking into account specific quality-of-service (QoS) constraints, where a decentralized algorithm was conceived for handling the constraint of limited information sharing among the base stations (BSs). In particular, the QoS multicast beamforming problem of terrestrial-satellite networks was studied in [20], while large-scale MIMO multicast beamforming aided non-cooperative cellular networks were studied in [21], where the pilot contamination problem was also considered.

Given the substantial benefits of relay-aided communications and multicast beamforming techniques, their joint design has attracted considerable attention [22]–[28]. Specifically, the cooperative multicast beamforming design of both single-antenna multi-relay (SAMR) and multi-antenna single-relay (MASR) scenarios were studied in [22] and [23], respectively. In [24], Li *et al.* put forward a cooperative multicast beamforming algorithm for multi-antenna multi-relay (MAMR) cognitive systems. Moreover, the network capacity bound of a twin-source multicast relay network was studied in [25] by Du *et al*. They also designed three relaying schemes based on network coding. In [26] and [27], the relaying schemes under user power constraints and per-antenna constraints were studied, respectively. Furthermore, Zhou *et al.* introduced a sophisticated relay selection scheme in [28], where the mobility of relay nodes was taken into account and a location-aware distributed relay selection method was proposed for improving

energy efficiency.

However, these state-of-the-art cooperative multicast beamforming schemes were designed for terrestrial communication systems, while there is a paucity of literature on maritime communication systems. Hence in this context the following differences have to be investigated, when designing multicast relaying systems:

- In contrast to terrestrial cellular networks, where the users are assumed to be rather densely and typically uniformly distributed in the coverage area, in maritime networks the users are clustered in ships, which are sparsely distributed on pre-set routes.

- The maritime relays tend to be distributed sparsely, resulting in long-distance hops. Moreover, the hostile propagation properties of the sea surface are rather unique.

- The energy constraints tend to be severe, since the off-shore relays are usually powered by solar energy.

Inspired by the aforementioned challenges, in this paper, we study the cooperative multicast problem of a coastal two-hop relaying system. Specifically, we intrinsically amalgamate MIMO and cooperative multicast beamforming techniques for supporting multimedia services for offshore vessel users. In our system, the base station ashore (BSA) and the offshore RNs cooperatively support downlink multimedia services. To the best of our knowledge, this is the first journal contribution on multicast relaying designed for maritime communication systems. Our main contributions are summarized as follows:

- By considering the specific characteristics of maritime channels and user distributions, we construct a realistic model for maritime multicast scenarios. Relying on the cooperation between the BSA and RNs, our cooperative multicast problem is formulated as a power minimization optimization problem under QoS constraints.

- A distributed beamforming optimization and relay design solution is derived with the aid of the feasible point pursuit successive convex approximation (FPP-SCA) approach. An alternating optimization (AO) algorithm is proposed, which yields a near-optimal solution to our power minimization problem. Furthermore, for the sake of further reducing the computational complexity, a low-complexity algorithm relying on zero-forcing (ZF) precoding is presented, followed by its closed-form solution.

- Extensive simulations are conducted for evaluating our proposed algorithms. Our simulation

results show the feasibility and efficiency of these algorithms, which are characterized by a fast convergence as well as an appealingly low power consumption.

The remainder of this paper is organized as follows. The system model and our cooperative multicast beamforming problem are elaborated on in Section II. In Section III, a distributed beamforming optimization and relay design solution as well as an AO algorithm are presented. A distributed low-complexity algorithm is proposed in Section IV. Numerical simulations are conducted in Section V, followed by our conclusions in Section VI.

Notations: In this paper, boldface uppercase letters and boldface lowercase letters denote matrices and column vectors, respectively. The superscripts $(\cdot)^*$, $(\cdot)^T$ and $(\cdot)^H$ denote the conjugate, the transpose and the Hermitian operation of a matrix or a vector, respectively. $|\cdot|$ denotes the absolute value of a complex number or the number of elements in a set, while $\|\cdot\|$ denotes the l_2 norm of a vector or the Frobenius norm of a matrix. $\mathsf{vec}\,(\cdot)$ represents the vectorization of a matrix and $\mathsf{BlkDiag}\,(\cdot)$ is the block diagonal concatenation of matrix input. $\mathsf{Tr}\,(\cdot)$ and $\mathsf{rank}\,(\cdot)$ return the trace and rank of a matrix, respectively. Moreover, $\boldsymbol{A} \in \mathbb{C}^{N_1 \times N_2}$ denotes that $\boldsymbol{A}$ is a complex matrix with the dimension of $N_1 \times N_2$, while $\boldsymbol{A}^\perp$ represents an orthogonal basis for the null space of $\boldsymbol{A}$. Furthermore, $\otimes$ denotes the Kronecker product and $\boldsymbol{I}_N$ is an $N \times N$ identity matrix. Finally, $\boldsymbol{x} \sim \mathcal{CN}\,(\boldsymbol{a}, \boldsymbol{B})$ represents a vector $\boldsymbol{x}$, which obeys the complex Gaussian distribution with a mean of $\boldsymbol{a}$ as well as a covariance matrix of $\boldsymbol{B}$.

II. System Model and Problem Formulation

In this section, we consider the downlink of a maritime multicast scenario including a single BSA, S RNs and a certain number of maritime users, as shown in Fig. 1. The set of S RNs is denoted as $\{RN_1, RN_2, ..., RN_S\}$. Moreover, since maritime users tend to be clustered by ships, we assume that the users in the same ship share the same multimedia services. The signals can be received as well as stored by the ship and then be transmitted to the users using WiFi. Hence the maritime users on board the same ship can be termed as vessel-based users equipped with a single antenna. By contrast, the BSA and the RNs are assumed to be equipped with N_B and N_R transmit antennas, respectively. All of the vessel-based users are divided into different groups depending on their QoS requirements and locations. For simplicity, each user can only be assigned to a single group during each scheduling interval. Without loss of generality, we assume that there are $(M + N)$ groups in total. Specifically, M groups near the shore are
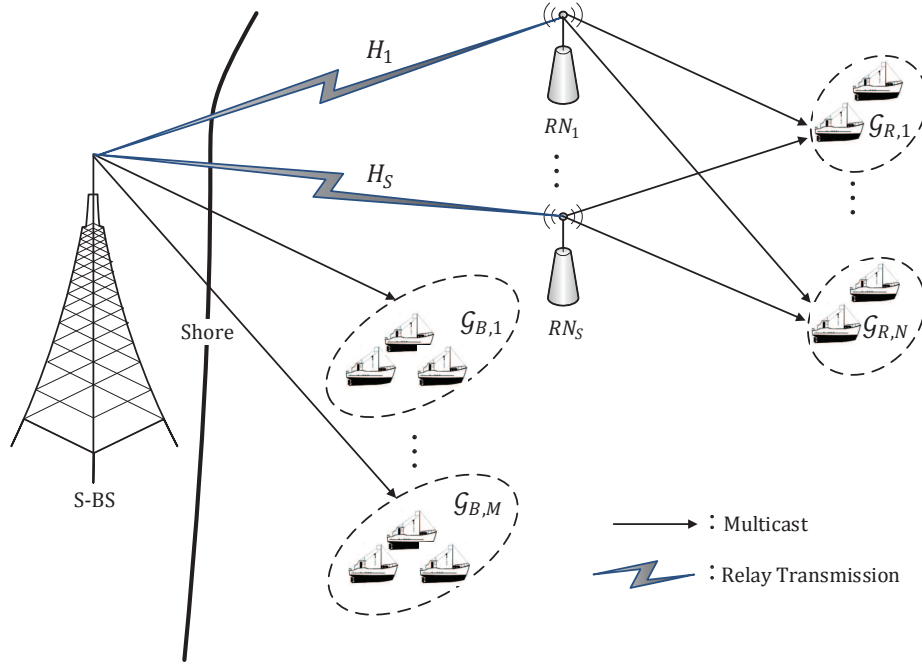
Fig. 1.   Illustration of a maritime multicast scenario including one S-BS, multiple RNs, and vessel users.

served directly by the BSA, while N offshore groups are served by the associated RN. Here we have $N_B \geq (M+N)$ and $N_R \geq N$. The M BS-aided groups and the N RN-assisted groups are denoted as $\{\mathcal{G}_{B,1}, \mathcal{G}_{B,2}, ..., \mathcal{G}_{B,M}\}$ and $\{\mathcal{G}_{R,1}, \mathcal{G}_{R,2}, ..., \mathcal{G}_{R,N}\}$, respectively. In the following, perfect channel state information (CSI) is assumed for simplicity. To boldly define our model:

$\boldsymbol{H}_s$ is the $N_B \times N_R$ complex channel vector between BSA and RN_s;

$\boldsymbol{h}_{m,i}$ is the $N_B \times 1$ complex channel vector between BSA and the ith user in $\mathcal{G}_{B,m}$;

$\boldsymbol{g}_{s,n,i}$ is the $N_R \times 1$ channel vector between RN_s and the ith user in $\mathcal{G}_{R,n}$;

$\boldsymbol{\omega}_{B,k}$ is beamforming vector of BSA for $\mathcal{G}_{B,k}$;

$\boldsymbol{\omega}_{R,k}$ is beamforming vector of BSA for $\mathcal{G}_{R,k}$;

$x_{B,k}$ is transmit message for $\mathcal{G}_{B,k}$ having $E\left[|x_{B,k}|^2\right] = 1$;

$x_{R,k}$ is the transmit message for $\mathcal{G}_{R,k}$ associated with $E\left[|x_{R,k}|^2\right] = 1$.

A. The Channel Model

Since the near-shore communication channel spans from a cellular tower to ships with less reflection from the sea-surface, the light-of-sight (LOS) path will be dominant. On the other hand, the second hop off-shore communication channel may substantially suffer from reflection by the sea surface, which may result in severe multipath effects. Therefore, in our model, an empirical loss Rician fading model is conceived for describing the first hop near-shore channel, which is given by [29]:

$$\boldsymbol{h} = d^{-\alpha/2}\boldsymbol{h}^f, \tag{1}$$

where d denotes the communication distance, α represents the path loss exponent and $\boldsymbol{h}^f$ denotes the small-scale channel fading coefficients. Additionally, a modified two-ray reflection model subject to Rayleigh fading is employed to describe the second hop off-shore channel [30], i.e. we have:

$$\boldsymbol{g} = \frac{\lambda}{4\pi d} \sin\left(\frac{2\pi h_t h_r}{\lambda d}\right) \boldsymbol{g}^f, \tag{2}$$

where λ, d, h_t, h_r denote the carrier wavelength, the communication distance, the height of the transmitter and the receiver, respectively, while $\boldsymbol{g}^f$ represents the small-scale fading coefficients.

B. The User Model

One of the main differences of our maritime communication systems compared to their terrestrial counterparts lies in that the users in the former are clustered by the ships, where each ship is regarded as a cluster head, while the users in the ship are cluster members. We assume that the users in the same ship are offered a menue of the same multimedia services to choose from, such as news bulletins, photos, audio and video clips, etc. This multimedia menue is firstly transmitted to the cluster head and then broadcast to the cluster members. Since all the users in the same ship share the same multimedia menue, we group them as vessel-users. Naturally, they also have the same QoS requirement. The QoS requirement is related to the distribution of the users, which is modeled by the so-called Thomas clustered process [31] in our model, where the users are assumed to be independent and identically distributed (i.i.d.) according to a symmetric normal distribution, with a variance of σ_u^2. The density function of the

user location is:

$$f_Y(y) = \frac{1}{2\pi\sigma_u^2} \exp(-\frac{\|y\|^2}{2\sigma_u^2}). \tag{3}$$

Furthermore, the distribution of intra-cluster distance between the cluster head and a cluster members is [32]:

$$f_L(l) = \frac{\frac{l}{\sigma_u^2} \exp(-\frac{l^2}{2\sigma_u^2})}{1 - \exp(-\frac{l_0^2}{2\sigma_u^2})}, \quad l \leq l_0. \tag{4}$$

C. The Signal Model

In our model, RNs operate in the amplify-and-forward (AF) aided half-duplex mode. In the first time slot, both the RNs and the BS-aided users receive their signal from the BSA. The received signal of RN_s and of the ith user in $\mathcal{G}_{B,m}$ can be expressed as:

$$\boldsymbol{y}_s = \boldsymbol{H}_s^H(\sum_{k=1}^{M}\boldsymbol{\omega}_{B,k}x_{B,k} + \sum_{k=1}^{N}\boldsymbol{\omega}_{R,k}x_{R,k}) + \boldsymbol{n}_s, \tag{5}$$

as well as:

$$y_{B,m,i} = \boldsymbol{h}_{m,i}^H(\sum_{k=1}^{M}\boldsymbol{\omega}_{B,k}x_{B,k} + \sum_{k=1}^{N}\boldsymbol{\omega}_{R,k}x_{R,k}) + n_{B,m,i}, \tag{6}$$

where $\boldsymbol{n}_s \sim \mathcal{CN}(0, \sigma_s^2\boldsymbol{I})$ and $n_{B,m,i} \sim \mathcal{CN}(0, \sigma_{B,m,i}^2)$ are additive white Gaussian noise (AWGN) processes. Hence, the received SINR of the ith user in $\mathcal{G}_{B,m}$ is given by:

$$\text{SINR}_{B,m,i} = \frac{\left|\boldsymbol{h}_{m,i}^H\boldsymbol{\omega}_{B,m}\right|^2}{\sum\limits_{k=1,k\neq m}^{M}\left|\boldsymbol{h}_{m,i}^H\boldsymbol{\omega}_{B,k}\right|^2 + \sum\limits_{k=1}^{N}\left|\boldsymbol{h}_{m,i}^H\boldsymbol{\omega}_{R,k}\right|^2 + \sigma_{B,m,i}^2}. \tag{7}$$

Furthermore, in the second time slot the signal received at the RN_s is processed by a $(N_R \times N_R)$ element relaying matrix of $\boldsymbol{W}_s$, and the resultant signal can be expressed as:

$$\boldsymbol{\tau}_s = \boldsymbol{W}_s\boldsymbol{H}_s^H(\sum_{k=1}^{M}\boldsymbol{\omega}_{B,k}x_{B,k} + \sum_{k=1}^{N}\boldsymbol{\omega}_{R,k}x_{R,k}) + \boldsymbol{W}_s\boldsymbol{n}_s. \tag{8}$$

Afterwards, it will be forwarded to the RN-assisted users. The received signal and the corresponding SINR of the ith user in $\mathcal{G}_{R,n}$ is given by:

$$y_{R,n,i} = \sum_{s=1}^{S}\boldsymbol{g}_{s,n,i}^H\boldsymbol{W}_s\boldsymbol{H}_s^H(\sum_{k=1}^{M}\boldsymbol{\omega}_{B,k}x_{B,k} + \sum_{k=1}^{N}\boldsymbol{\omega}_{R,k}x_{R,k}) + \sum_{s=1}^{S}\boldsymbol{g}_{s,n,i}^H\boldsymbol{W}_s\boldsymbol{n}_s + n_{R,n,i}, \tag{9}$$

and

$$\text{SINR}_{R,n,i} =$$

$$\frac{\left| \sum\limits_{s=1}^{S} \boldsymbol{g}_{s,n,i}^{H} \boldsymbol{W}_s \boldsymbol{H}_s^{H} \boldsymbol{\omega}_{R,n} \right|^2}{\sum\limits_{k=1}^{M} \left| \sum\limits_{s=1}^{S} \boldsymbol{g}_{s,n,i}^{H} \boldsymbol{W}_s \boldsymbol{H}_s^{H} \boldsymbol{\omega}_{B,k} \right|^2 + \sum\limits_{k=1,k\neq n}^{N} \left| \sum\limits_{s=1}^{S} \boldsymbol{g}_{s,n,i}^{H} \boldsymbol{W}_s \boldsymbol{H}_s^{H} \boldsymbol{\omega}_{R,k} \right|^2 + \sum\limits_{s=1}^{S} \sigma_s^2 \left\| \boldsymbol{g}_{s,n,i}^{H} \boldsymbol{W}_s \right\|^2 + \sigma_{R,n,i}^2},$$

$$(10)$$

respectively, where $n_{R,n,i} \sim \mathcal{CN}(0, \sigma_{R,n,i}^2)$ is the AWGN.

Hence, the total transmit power of the multicast system can be calculated as:

$$P_{\text{total}} = \sum_{k=1}^{M} \|\boldsymbol{\omega}_{B,k}\|^2 + \sum_{k=1}^{N} \|\boldsymbol{\omega}_{R,k}\|^2 + \sum_{s=1}^{S}\sum_{k=1}^{M} \left\| \boldsymbol{W}_s \boldsymbol{H}_s^{H} \boldsymbol{\omega}_{B,k} \right\|^2 + \sum_{s=1}^{S}\sum_{k=1}^{N} \left\| \boldsymbol{W}_s \boldsymbol{H}_s^{H} \boldsymbol{\omega}_{R,k} \right\|^2$$
$$+ \sum_{s=1}^{S} \sigma_s^2 \|\boldsymbol{W}_s\|^2,$$

$$(11)$$

where the first two terms are the power consumption of BSA, while the latter three terms represent the total power consumption of S RNs.

D. Problem Formulation

Since maritime communication systems usually face with severe power limit for lacking stable power sources, our objective is to minimize the total transmit power of the whole system with respect to a given set of received SINR constraint for each group, by jointly designing $\{\boldsymbol{\omega}_{B,k}, \boldsymbol{\omega}_{R,k}\}$ and $\{\boldsymbol{W}_s\}$. Let the received SINR targets of the users in $\mathcal{G}_{B,m}$ and $\mathcal{G}_{R,n}$ be $\gamma_{B,m}$ and $\gamma_{R,n}$, respectively. Then the multicast problem can be formulated as:

$$\min_{\{\boldsymbol{\omega}_{B,k}, \boldsymbol{\omega}_{R,k}, \boldsymbol{W}_s\}} P_{\text{total}} \tag{12}$$

$$\text{s.t.} \quad \text{SINR}_{B,m,i} \geq \gamma_{B,m}, \forall m, i \in \mathcal{G}_{B,m}, \tag{12a}$$

$$\text{SINR}_{R,n,i} \geq \gamma_{R,n}, \forall n, i \in \mathcal{G}_{R,n}. \tag{12b}$$

E. Discussion on the SINR Targets

As mentioned in Section II-B, since the users in the same ship constitute a cluster, the SINR targets have to be carefully chosen for satisfying all the users. Without loss of generality, in the

following, we only consider a single cluster as a simple example and study how to choose the SINR target. The SINR target mainly depends on the total throughput required by all the users and on the intra-cluster link quality. Assuming that the arrival of data requirements from all the users in the cluster considered can be modeled by a Poisson process with arrival rate λ and that the average successful transmission probability of an intra-cluster link is $\bar{p}$, the SINR target of this cluster can be expressed as:

$$\gamma^{\text{th}} = 2^{\frac{\lambda}{\bar{p}}} - 1, \tag{13}$$

where $\bar{p}$ can be derived by averaging the successful transmission probability of the users. Assuming that the channel between the cluster head and a cluster member is a Rayleigh fading channel having a unit mean, $\bar{p}$ can be calculated as:

$$
\begin{aligned}
\bar{p} &= \int_0^{l_0} \exp(-\frac{\gamma^{\text{M}}}{P^{\text{H}}} l^{\frac{\alpha}{2}}) f_L(l) \mathrm{d}l \\
&= \frac{\int_0^{l_0} \exp(-\frac{\gamma^{\text{M}}}{P^{\text{H}}} l^{\frac{\alpha}{2}}) \frac{l}{\sigma_u^2} \exp(-\frac{l^2}{2\sigma_u^2})}{1 - \exp(-\frac{l_0^2}{2\sigma_u^2})},
\end{aligned}
\tag{14}
$$

where P^{H} and γ^{M} represent the transmit power of the cluster head and the receiving threshold of the cluster member, respectively. Bearing in mind that a multicast group consists of multiple clusters, the SINR targets can be set equal to the maximum of the group, i.e. we have $\gamma_{B,m} = \max_{i \in \mathcal{G}_{B,m}} \{\gamma_i^{\text{th}}\}$.

III. Joint Beamforming and Relay Design

The problem in (12) is a continuous variable optimization problem, which cannot be handled by the excessive-complexity Brute-force search. Considering the structure and non-convex nature of the problem, in the following, we use an AO method to solve it. In Section III, we first fix the BSA beamforming vectors $\{\boldsymbol{\omega}_{B,k}, \boldsymbol{\omega}_{R,k}\}$ and design the RNs' processing matrices $\{\boldsymbol{W}_s\}$. Then, relying on the RNs' processing matrices $\{\boldsymbol{W}_s\}$ obtained, we optimize the BSA beamforming vectors. After that, we propose an AO algorithm to find the solution to (12). Furthermore, in Section IV, we derive a closed-form solution based on ZF precoding for further reducing the complexity.

A. Processing Matrices Design of RNs

Given the BSA beamforming vectors $\{\boldsymbol{\omega}_{B,k}, \boldsymbol{\omega}_{R,k}\}$, by removing the constant terms, the optimization objective in (12) can be reduced to:

$$P_{\text{total}}^{[1]} = \sum_{s=1}^{S}\sum_{k=1}^{M}\left\|\boldsymbol{W}_s\boldsymbol{H}_s^H\boldsymbol{\omega}_{B,k}\right\|^2 + \sum_{s=1}^{S}\sum_{k=1}^{N}\left\|\boldsymbol{W}_s\boldsymbol{H}_s^H\boldsymbol{\omega}_{R,k}\right\|^2 + \sum_{s=1}^{S}\sigma_s^2\|\boldsymbol{W}_s\|^2. \tag{15}$$

Furthermore, since the change of $\{\boldsymbol{W}_s\}$ does not affect the received SINR of BS-aided users, (12) can be reformulated as:

$$\min_{\{\boldsymbol{W}_s\}} \quad P_{\text{total}}^{[1]} \tag{16}$$

$$\text{s.t.} \quad \text{SINR}_{R,n,i} \geq \gamma_{R,n}, \forall n, i \in \mathcal{G}_{R,n}. \tag{16a}$$

Theorem 1. *Defining* $\boldsymbol{r}_{s,k} \triangleq \boldsymbol{H}_s^H\boldsymbol{\omega}_{R,k}$ *and* $\boldsymbol{R}_s \triangleq [\boldsymbol{r}_{s,1}, ..., \boldsymbol{r}_{s,N}]$, *the optimal processing matrix* $\boldsymbol{W}_s$ *of* RN_s *is given by:*

$$\boldsymbol{W}_s = \boldsymbol{V}_s\boldsymbol{R}_s^H, \tag{17}$$

where $\boldsymbol{V}_s \triangleq [\boldsymbol{v}_{s,1}, ..., \boldsymbol{v}_{s,N}] \in \mathbb{C}^{N_R \times N}$.

Proof: See Appendix A. ∎

Remark 1. Theorem 1 indicates that $\boldsymbol{W}_s$ can be divided into two parts, i.e. $\boldsymbol{V}_s$ and $\boldsymbol{R}_s^H$. Correspondingly, the relay process of RN_s can be divided into two phases, as shown in Fig. 2, where RN_s first receives the source signals using a multi-stream matched-filter receiver $\boldsymbol{R}_s^H$ in Phase I, and then transmits the processed signals to the vessel users relying on relaying vectors $[\boldsymbol{v}_{s,1}, ..., \boldsymbol{v}_{s,N}]$ in Phase II.

Remark 2. Theorem 1 is an extension of the case where there is only one multi-antenna relay node and one multi-antenna receiver [33]–[36]. Let the beamforming vector of the source be $\boldsymbol{s}$, while the channel vectors between the source and the relay, the relay and the receiver be $\boldsymbol{H}_1$ and $\boldsymbol{H}_2$, respectively. Then, the matching design of the RN's processing matrix can be achieved. To elaborate, the RN first maximizes the received SNR by matching the effective channel $\boldsymbol{H}_1\boldsymbol{s}$, and then transmits the signal through the dominant right singular vector of $\boldsymbol{H}_2$. The optimality of the matching design at the RNs was shown in [36].
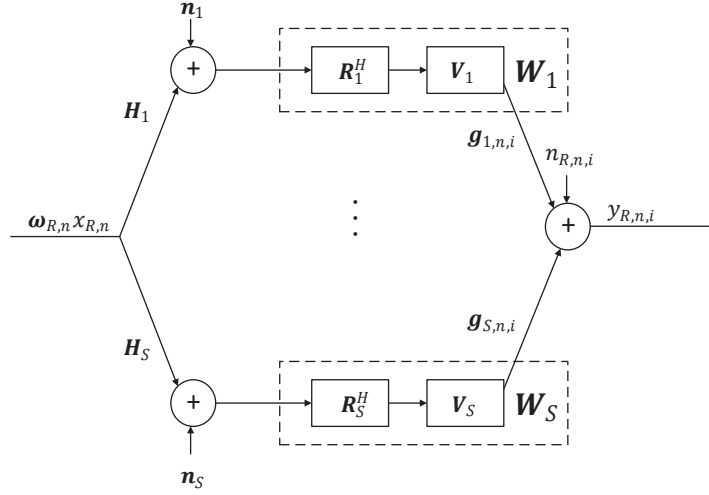
Fig. 2. Illustration of the relaying process at the RNs

Based on Theorem 1, the optimization problem of $\{W_s\}$ can be converted into optimizing $\{V_s\}$, since $\{R_s^H\}$ are already known. Since $N_R \geq N$, the number of variables in (16) reduces from SN_R^2 to SN_RN. Substituting W_s with $V_sR_s^H$ and defining $\phi_{s,k} \triangleq R_s^H H_s^H \omega_{B,k}$, $\psi_{s,k} \triangleq R_s^H r_{s,k}$, the optimization objective in (16) becomes:

$$P_{\text{total}}^{[1]} = \sum_{s=1}^{S}\sum_{k=1}^{M} \|V_s\phi_{s,k}\|^2 + \sum_{s=1}^{S}\sum_{k=1}^{N} \|V_s\psi_{s,k}\|^2 + \sum_{s=1}^{S} \sigma_s^2\|V_sR_s^H\|^2. \tag{18}$$

Let us define:

$$\begin{cases} \Phi_s = [\phi_{s,1}, ..., \phi_{s,M}], \\ \Psi_s = [\psi_{s,1}, ..., \psi_{s,N}]. \end{cases} \tag{19}$$

Then (18) can be rewritten as:

$$\begin{aligned} P_{\text{total}}^{[1]} &= \sum_{s=1}^{S} \mathsf{Tr}\left[V_s\left(\Phi_s\Phi_s^H + \Psi_s\Psi_s^H + \sigma_s^2 R_s^H R_s\right) V_s^H\right] \\ &= \sum_{s=1}^{S} v_s^T Q_s v_s^*, \end{aligned} \tag{20}$$

where

$$\begin{cases} v_s \triangleq \mathsf{vec}(V_s^T), \\ Q_s \triangleq I_{N_R} \otimes (\Phi_s\Phi_s^H + \Psi_s\Psi_s^H + \sigma_s^2 R_s^H R_s). \end{cases} \tag{21}$$

Similarly, substituting $\boldsymbol{\phi}_{s,k}$ and $\boldsymbol{\psi}_{s,k}$ into (10) and using $\text{vec}(\boldsymbol{A}_1\boldsymbol{A}_2\boldsymbol{A}_3) = (\boldsymbol{A}_3^T \otimes \boldsymbol{A}_1)\text{vec}(\boldsymbol{A}_2)$, we have:

$$\begin{cases} \boldsymbol{g}_{s,n,i}^H \boldsymbol{V}_s \boldsymbol{\phi}_{s,k} = \hat{\boldsymbol{g}}_{k,s,n,i}^H \boldsymbol{v}_s, \\ \boldsymbol{g}_{s,n,i}^H \boldsymbol{V}_s \boldsymbol{\psi}_{s,k} = \tilde{\boldsymbol{g}}_{k,s,n,i}^H \boldsymbol{v}_s, \\ \boldsymbol{g}_{s,n,i}^H \boldsymbol{V}_s \boldsymbol{R}_s^H = \boldsymbol{G}_{s,n,i} \boldsymbol{v}_s, \end{cases} \tag{22}$$

where

$$\begin{cases} \hat{\boldsymbol{g}}_{k,s,n,i} \triangleq \boldsymbol{g}_{s,n,i} \otimes \boldsymbol{\phi}_{s,k}^*, \\ \tilde{\boldsymbol{g}}_{k,s,n,i} \triangleq \boldsymbol{g}_{s,n,i} \otimes \boldsymbol{\psi}_{s,k}^*, \\ \boldsymbol{G}_{s,n,i}(j,:) \triangleq \boldsymbol{g}_{s,n,i}^H \otimes \boldsymbol{R}_s^*(j,:). \end{cases} \tag{23}$$

According to (22), the received SINR in (10) can be rewritten as:

$$\text{SINR}_{R,n,i} = \frac{\left| \sum_{s=1}^{S} \tilde{\boldsymbol{g}}_{n,s,n,i}^H \boldsymbol{v}_s \right|^2}{\sum_{k=1}^{M} \left| \sum_{s=1}^{S} \hat{\boldsymbol{g}}_{k,s,n,i}^H \boldsymbol{v}_s \right|^2 + \sum_{k=1,k\neq n}^{N} \left| \sum_{s=1}^{S} \tilde{\boldsymbol{g}}_{k,s,n,i}^H \boldsymbol{v}_s \right|^2 + \sum_{s=1}^{S} \sigma_s^2 \|\boldsymbol{G}_{s,n,i} \boldsymbol{v}_s\|^2 + \sigma_{R,n,i}^2}. \tag{24}$$

Upon combining (20) and (24), the optimization problem in (16) can be rewritten as:

$$\min_{\{\boldsymbol{v}_s\}} \quad \sum_{s=1}^{S} \boldsymbol{v}_s^T \boldsymbol{Q}_s \boldsymbol{v}_s^* \tag{25}$$

$$\text{s.t.} \quad \text{SINR}_{R,n,i} \geq \gamma_{R,n}, \forall n, i \in \mathcal{G}_{R,n}. \tag{25a}$$

Moreover, by defining:

$$\begin{cases} \boldsymbol{v} \triangleq \left[\boldsymbol{v}_1^T, ..., \boldsymbol{v}_S^T\right]^T, \\ \boldsymbol{Q} \triangleq \text{BlkDiag}(\boldsymbol{Q}_1, ..., \boldsymbol{Q}_S), \\ \tilde{\boldsymbol{f}}_{k,n,i} \triangleq \left[\tilde{\boldsymbol{g}}_{k,1,n,i}^T, ..., \tilde{\boldsymbol{g}}_{k,S,n,i}^T\right]^T, \\ \hat{\boldsymbol{f}}_{k,n,i} \triangleq \left[\hat{\boldsymbol{g}}_{k,1,n,i}^T, ..., \hat{\boldsymbol{g}}_{k,S,n,i}^T\right]^T, \\ \boldsymbol{G}_{n,i} \triangleq \text{BlkDiag}(\sigma_1 \boldsymbol{G}_{1,n,i}, ..., \sigma_S \boldsymbol{G}_{S,n,i}), \end{cases} \tag{26}$$

(25) can be further reformulated as:

$$\min_{\{v\}} \quad v^T Q v^* \tag{27}$$

$$\text{s.t.} \quad \frac{\left|\tilde{f}_{n,n,i}^H v\right|^2}{\sum_{k=1}^{M}\left|\hat{f}_{k,n,i}^H v\right|^2 + \sum_{k=1,k\neq n}^{N}\left|\tilde{f}_{k,n,i}^H v\right|^2 + \|G_{n,i}v\|^2 + \sigma_{R,n,i}^2} \geq \gamma_{R,n}, \forall n, i \in \mathcal{G}_{R,n}. \tag{27a}$$

We have now transformed the problem in (16) into the more straightforward form as in (27). However, unfortunately the constraints in (27a) are still non-convex. Existing techniques usually relax the non-convex problem using semi-definite relaxation (SDR) or linearize the non-convex part [37]. However, sometimes both the methods fail to arrive at a feasible solution. Here we invoke a novel approach termed as FPP-SCA to solve the problem. Explicitly, the FPP-SCA approach linearizes the non-convex parts of the problem as conventional SCA does, but adds some slack variables to sustain feasibility [38]. By introducing a slack variable ρ_R, (27) can be transformed into the following equivalent problem:

$$\min_{\{v\}} \quad \rho_R \tag{28}$$

$$\text{s.t.} \quad v^T Q v^* \leq \rho_R, \tag{28a}$$

$$\sum_{k=1}^{M}\gamma_{R,n}\left|\hat{f}_{k,n,i}^H v\right|^2 + \sum_{k=1,k\neq n}^{N}\gamma_{R,n}\left|\tilde{f}_{k,n,i}^H v\right|^2 + \gamma_{R,n}\|G_{n,i}v\|^2$$

$$- \left|\tilde{f}_{n,n,i}^H v\right|^2 \leq -\gamma_{R,n}\sigma_{R,n,i}^2, \quad \forall n, i \in \mathcal{G}_{R,n}. \tag{28b}$$

In order to invoke successive convex approximation, we let:

$$v^H\left(\Lambda_{R,n,i}^+ + \Lambda_{R,n,i}^-\right)v$$

$$= \sum_{k=1}^{M}\gamma_{R,n}\left|\hat{f}_{k,n,i}^H v\right|^2 + \sum_{k=1,k\neq n}^{N}\gamma_{R,n}\left|\tilde{f}_{k,n,i}^H v\right|^2 + \gamma_{R,n}\|G_{n,i}v\|^2 - \left|\tilde{f}_{n,n,i}^H v\right|^2, \tag{29}$$

where we have $\Lambda_{R,n,i}^+ \succeq 0$, $\Lambda_{R,n,i}^- \preceq 0$ and they are defined by:

$$\begin{cases} \Lambda_{R,n,i}^+ \triangleq \sum_{k=1}^{M}\gamma_{R,n}\hat{f}_{k,n,i}\hat{f}_{k,n,i}^H + \sum_{k=1,k\neq n}^{N}\gamma_{R,n}\tilde{f}_{k,n,i}\tilde{f}_{k,n,i}^H + \gamma_{R,n}G_{n,i}^H G_{n,i}, \\ \Lambda_{R,n,i}^- \triangleq -\tilde{f}_{n,n,i}\tilde{f}_{n,n,i}^H. \end{cases} \tag{30}$$

Since $\Lambda_{R,n,i}^-$ is negative semi-definite, for any $z \in \mathbb{C}^{SN_RN\times1}$, we have:

$$(v - z)^H \Lambda_{R,n,i}^- (v - z)$$
$$= v^H \Lambda_{R,n,i}^- v - 2\text{Re}\left\{z^H \Lambda_{R,n,i}^- v\right\} + z^H \Lambda_{R,n,i}^- z \leq 0. \tag{31}$$

Inequality (31) refers to a linear restriction around the point z. Then, relying on the FPP-SCA as well as on the inequality (31), the non-convex constraints in (28b) can be substituted by a convex constraint as follows:

$$v^H \Lambda_{R,n,i}^+ v + 2\text{Re}\left\{z^H \Lambda_{R,n,i}^- v\right\} \leq z^H \Lambda_{R,n,i}^- z - \gamma_{R,n}\sigma_{R,n,i}^2 + \epsilon_{R,n,i}, \tag{32}$$

where $\epsilon_{R,n,i}$ is a slack penalty variable proposed in FPP-SCA to ensure the feasibility of the problem. According to FPP-SCA, we can use an iterative algorithm to obtain the near-optimal value of v, where the optimization problem to be solved at the kth iteration is given by:

$$\min_{v} \quad \rho_R + C\|\boldsymbol{\epsilon}\| \tag{33}$$

$$\text{s.t.} \quad v^T Q v^* \leq \rho_R, \tag{33a}$$

$$v^H \Lambda_{R,n,i}^+ v + 2\text{Re}\left\{z_k^H \Lambda_{R,n,i}^- v\right\}$$
$$\leq z_k^H \Lambda_{n,i}^- z_k - \gamma_{R,n}\sigma_{R,n,i}^2 + \epsilon_{R,n,i}, \forall n, i \in \mathcal{G}_{R,n}, \tag{33b}$$

$$\epsilon_{R,n,i} \geq 0, \forall n, i \in \mathcal{G}_{R,n}, \tag{33c}$$

where $\boldsymbol{\epsilon} = \left[\epsilon_{R,1,1}, ..., \epsilon_{R,N,|\mathcal{G}_{R,N}|}\right]^T$ and C is the penalty coefficient. We let $C \gg 1$ to force the slack penalty variables toward zero for ensuring that the final solution is feasible to (28). Furthermore, z_k is set to be equal to the optimal v obtained in the $(k-1)$st iteration, while the initial point z_0 is randomly generated. By now, a near-optimal solution $\hat{v}$ to (28) has been found. When we have $\hat{v}$, the optimal $\{\hat{W}_s\}$ associated with $\{\omega_{B,k}, \omega_{R,k}\}$ can be obtained.

B. Beamforming Optimization for the BSA

In Section III-A, the optimization problem of $\{W_s\}$ has been transformed into the relaying vector design of $\{V_s\}$ for employment at the RNs relying on Theorem 1, which can be efficiently solved by the FPP-SCA approach. In this section, we focus our attention on the design of the BSA beamforming vectors $\{\omega_{B,k}, \omega_{R,k}\}$ based on the processing matrices obtained.

Let us denote the processing matrices obtained in Section III-A as $\{\hat{\boldsymbol{W}}_s\}$. By ignoring the constant terms, the optimization objective in (12) can be reduced to:

$$P_{\text{total}}^{[2]} = \sum_{k=1}^{M} \|\boldsymbol{\omega}_{B,k}\|^2 + \sum_{k=1}^{N} \|\boldsymbol{\omega}_{R,k}\|^2 + \sum_{s=1}^{S}\sum_{k=1}^{M} \left\|\hat{\boldsymbol{W}}_s\boldsymbol{H}_s^H\boldsymbol{\omega}_{B,k}\right\|^2 + \sum_{s=1}^{S}\sum_{k=1}^{N} \left\|\hat{\boldsymbol{W}}_s\boldsymbol{H}_s^H\boldsymbol{\omega}_{R,k}\right\|^2.$$

$$(34)$$

Furthermore, let $\boldsymbol{W}_s = \hat{\boldsymbol{W}}_s$. Then the SINRs have the same expressions as (7) and (12). Hence, the optimization problem in (10) can be rewritten as:

$$\min_{\{\boldsymbol{\omega}_{B,k},\boldsymbol{\omega}_{R,k}\}} \quad P_{\text{total}}^{[2]} \tag{35}$$

$$\text{s.t.} \quad \text{SINR}_{B,m,i} \geq \gamma_{R,m}, \forall m, i \in \mathcal{G}_{B,m}, \tag{35a}$$

$$\text{SINR}_{R,n,i} \geq \gamma_{R,n}, \forall n, i \in \mathcal{G}_{R,n}. \tag{35b}$$

Upon defining:

$$\begin{cases} \boldsymbol{g}_{n,i} \triangleq \sum_{s=1}^{S} \boldsymbol{H}_s\hat{\boldsymbol{W}}_s^H\boldsymbol{g}_{s,n,i}, \\ \tilde{\sigma}_{R,n,i}^2 \triangleq \sum_{s=1}^{S} \sigma_s^2\left\|\boldsymbol{g}_{s,n,i}^H\hat{\boldsymbol{W}}_s\right\|^2 + \sigma_{R,n,i}^2, \end{cases} \tag{36}$$

(35) can be reformulated as:

$$\min_{\{\boldsymbol{\omega}_{B,k},\boldsymbol{\omega}_{R,k}\}} \quad P_{\text{total}}^{[2]} \tag{37}$$

$$\text{s.t.} \quad \frac{\left|\boldsymbol{h}_{m,i}^H\boldsymbol{\omega}_{B,m}\right|^2}{\sum\limits_{k=1,k\neq m}^{M} \left|\boldsymbol{h}_{m,i}^H\boldsymbol{\omega}_{B,k}\right|^2 + \sum\limits_{k=1}^{N} \left|\boldsymbol{h}_{m,i}^H\boldsymbol{\omega}_{R,k}\right|^2 + \sigma_{B,m,i}^2} \geq \gamma_{B,m}, \forall m, i \in \mathcal{G}_{B,m}, \tag{37a}$$

$$\frac{\left|\boldsymbol{g}_{n,i}^H\boldsymbol{\omega}_{R,n}\right|^2}{\sum\limits_{k=1}^{M} \left|\boldsymbol{g}_{n,i}^H\boldsymbol{\omega}_{B,k}\right|^2 + \sum\limits_{k=1,k\neq n}^{N} \left|\boldsymbol{g}_{n,i}^H\boldsymbol{\omega}_{R,k}\right|^2 + \tilde{\sigma}_{R,n,i}^2} \geq \gamma_{R,n}, \forall n, i \in \mathcal{G}_{R,n}. \tag{37b}$$

By observing (37) we can see that given the processing matrices $\{\hat{\boldsymbol{W}}_s\}$ of the RNs, the RN-assisted users can be viewed as BS-aided users, and the channel vector between the BSA and the ith user in $\{\mathcal{G}_{R,n}\}$ can be modeled as $\boldsymbol{g}_{n,i}$. However, problem in (37) is still not convex. Once again, the FPP-SCA approach is invoked for solving the problem. We first introduce a

slack variable ρ_B, and convert (37) into an equivalent problem, which can be formulated as:

$$\min_{\{\boldsymbol{\omega}_{B,k}, \boldsymbol{\omega}_{R,k}\}} \rho_B \tag{38}$$

$$\text{s.t.} \quad P_{\text{total}}^{[2]} \le \rho_B, \tag{38a}$$

$$\sum_{k=1,k\ne m}^{M} \gamma_{B,m} \left| \boldsymbol{h}_{m,i}^{H} \boldsymbol{\omega}_{B,k} \right|^2 + \sum_{k=1}^{N} \gamma_{B,m} \left| \boldsymbol{h}_{m,i}^{H} \boldsymbol{\omega}_{R,k} \right|^2 - \left| \boldsymbol{h}_{m,i}^{H} \boldsymbol{\omega}_{B,m} \right|^2$$

$$\le -\gamma_{B,m} \sigma_{B,m,i}^2, \forall m, i \in \mathcal{G}_{B,m}, \tag{38b}$$

$$\sum_{k=1}^{M} \gamma_{R,n} \left| \boldsymbol{g}_{n,i}^{H} \boldsymbol{\omega}_{B,k} \right|^2 + \sum_{k=1,k\ne n}^{N} \gamma_{R,n} \left| \boldsymbol{g}_{n,i}^{H} \boldsymbol{\omega}_{R,k} \right|^2 - \left| \boldsymbol{g}_{n,i}^{H} \boldsymbol{\omega}_{R,n} \right|^2$$

$$\le -\gamma_{R,n} \tilde{\sigma}_{R,n,i}^2, \forall n, i \in \mathcal{G}_{R,n}. \tag{38c}$$

We then change the optimization variables from $\{\boldsymbol{\omega}_{B,k}, \boldsymbol{\omega}_{R,k}\}$ to $\boldsymbol{\omega} = \left[\boldsymbol{\omega}_{B,1}^T, ..., \boldsymbol{\omega}_{B,M}^T, \boldsymbol{\omega}_{R,1}^T, ..., \boldsymbol{\omega}_{R,N}^T \right]^T$. By defining:

$$\boldsymbol{\Theta} \triangleq \boldsymbol{I}_{M+N} \otimes \left(\sum_{s=1}^{S} \boldsymbol{H}_s \boldsymbol{W}_s^H \boldsymbol{W}_s \boldsymbol{H}_s^H \right), \tag{39}$$

$P_{\text{total}}^{[2]}$ can be expressed as:

$$P_{\text{total}}^{[2]} = \boldsymbol{\omega}^H \boldsymbol{\omega} + \boldsymbol{\omega}^H \boldsymbol{\Theta} \boldsymbol{\omega}. \tag{40}$$

Similarly, we let:

$$\boldsymbol{\omega}^H \left(\boldsymbol{\Gamma}_{B,m,i}^+ + \boldsymbol{\Gamma}_{B,m,i}^- \right) \boldsymbol{\omega} = \sum_{k=1,k\ne m}^{M} \gamma_{B,m} \left| \boldsymbol{h}_{m,i}^H \boldsymbol{\omega}_{B,k} \right|^2 + \sum_{k=1}^{N} \gamma_{B,m} \left| \boldsymbol{h}_{m,i}^H \boldsymbol{\omega}_{R,k} \right|^2 - \left| \boldsymbol{h}_{m,i}^H \boldsymbol{\omega}_{B,m} \right|^2, \tag{41}$$

$$\boldsymbol{\omega}^H \left(\boldsymbol{\Gamma}_{R,n,i}^+ + \boldsymbol{\Gamma}_{R,n,i}^- \right) \boldsymbol{\omega} = \sum_{k=1}^{M} \gamma_{R,n} \left| \boldsymbol{g}_{n,i}^H \boldsymbol{\omega}_{B,k} \right|^2 + \sum_{k=1,k\ne n}^{N} \gamma_{R,n} \left| \boldsymbol{g}_{n,i}^H \boldsymbol{\omega}_{R,k} \right|^2 - \left| \boldsymbol{g}_{n,i}^H \boldsymbol{\omega}_{R,n} \right|^2, \tag{42}$$

where $\boldsymbol{\Gamma}_{B,m,i}^+$, $\boldsymbol{\Gamma}_{B,m,i}^-$, $\boldsymbol{\Gamma}_{R,n,i}^-$ and $\boldsymbol{\Gamma}_{R,n,i}^-$ are defined by:

$$\begin{cases} \boldsymbol{\Gamma}_{B,m,i}^+ \triangleq \gamma_{B,m} \boldsymbol{I}_{M+N,\overline{m}} \otimes \left(\boldsymbol{h}_{m,i} \boldsymbol{h}_{m,i}^H \right), \\[2mm] \boldsymbol{\Gamma}_{B,m,i}^- \triangleq \left(\boldsymbol{I}_{M+N,\overline{m}} - \boldsymbol{I}_{M+N} \right) \otimes \left(\boldsymbol{h}_{m,i} \boldsymbol{h}_{m,i}^H \right), \\[2mm] \boldsymbol{\Gamma}_{R,n,i}^+ \triangleq \gamma_{R,n} \boldsymbol{I}_{M+N,\overline{M+n}} \otimes \left(\boldsymbol{g}_{n,i} \boldsymbol{g}_{n,i}^H \right), \\[2mm] \boldsymbol{\Gamma}_{R,n,i}^- \triangleq \left(\boldsymbol{I}_{M+N,\overline{M+n}} - \boldsymbol{I}_{M+N} \right) \otimes \left(\boldsymbol{g}_{n,i} \boldsymbol{g}_{n,i}^H \right), \end{cases} \tag{43}$$

where the diagonal matrix $\boldsymbol{I}_{M+N,\overline{m}}$ is obtained by setting the mth diagonal elements of $\boldsymbol{I}_{M+N}$ to zero. Then, the non-convex constraints in (38b) and (38c) can be substituted by the convex constraints as follows:

$$\boldsymbol{\omega}^{H}\boldsymbol{\Gamma}_{B,m,i}^{+}\boldsymbol{\omega} + 2\text{Re}\left\{\boldsymbol{z}^{H}\boldsymbol{\Gamma}_{B,m,i}^{-}\boldsymbol{\omega}\right\} \leq \boldsymbol{z}^{H}\boldsymbol{\Gamma}_{B,m,i}^{-}\boldsymbol{z} - \gamma_{B,m}\sigma_{B,m,i}^{2} + \epsilon_{B,m,i}, \tag{44}$$

$$\boldsymbol{\omega}^{H}\boldsymbol{\Gamma}_{R,n,i}^{+}\boldsymbol{\omega} + 2\text{Re}\left\{\boldsymbol{z}^{H}\boldsymbol{\Gamma}_{R,n,i}^{-}\boldsymbol{\omega}\right\} \leq \boldsymbol{z}^{H}\boldsymbol{\Gamma}_{R,n,i}^{-}\boldsymbol{z} - \gamma_{R,n}\tilde{\sigma}_{B,n,i}^{2} + \epsilon_{R,n,i}, \tag{45}$$

where $\epsilon_{B,m,i}$ and $\epsilon_{R,n,i}$ are slack penalty variables. According to FPP-SCA, combining (40), (44) and (45), we can use an iterative algorithm for finding the near-optimal value of $\boldsymbol{\omega}$, where the optimization problem to be solved at the kth iteration is expressed as:

$$\min_{\boldsymbol{\omega}} \quad \rho_{B} + C\|\boldsymbol{\epsilon}\|_{2} \tag{46}$$

$$\text{s.t.} \quad \boldsymbol{\omega}^{H}\boldsymbol{\omega} + \boldsymbol{\omega}^{H}\boldsymbol{\Theta}\boldsymbol{\omega} \leq \rho_{B}, \tag{46a}$$

$$\boldsymbol{\omega}^{H}\boldsymbol{\Gamma}_{B,m,i}^{+}\boldsymbol{\omega} + 2\text{Re}\left\{\boldsymbol{z}_{k}^{H}\boldsymbol{\Gamma}_{B,m,i}^{-}\boldsymbol{\omega}\right\} \tag{46b}$$

$$\leq \boldsymbol{z}_{k}^{H}\boldsymbol{\Gamma}_{B,m,i}^{-}\boldsymbol{z}_{k} - \gamma_{B,m}\sigma_{B,m,i}^{2} + \epsilon_{B,m,i}, \forall m, i \in \mathcal{G}_{B,m},$$

$$\boldsymbol{\omega}^{H}\boldsymbol{\Gamma}_{R,n,i}^{+}\boldsymbol{\omega} + 2\text{Re}\left\{\boldsymbol{z}_{k}^{H}\boldsymbol{\Gamma}_{R,n,i}^{-}\boldsymbol{\omega}\right\} \tag{46c}$$

$$\leq \boldsymbol{z}_{k}^{H}\boldsymbol{\Gamma}_{R,n,i}^{-}\boldsymbol{z}_{k} - \gamma_{R,n}\tilde{\sigma}_{B,n,i}^{2} + \epsilon_{R,n,i}, \forall n, i \in \mathcal{G}_{R,n},$$

$$\epsilon_{B,m,i} \geq 0, \forall m, i \in \mathcal{G}_{B,m}, \quad \epsilon_{R,n,i} \geq 0, \forall n, i \in \mathcal{G}_{R,n}, \tag{46d}$$

where $\boldsymbol{\epsilon} = \left[\epsilon_{B,1,1}, ..., \epsilon_{B,M,|\mathcal{G}_{B,M}|}, \epsilon_{R,1,1}, ..., \epsilon_{R,N,|\mathcal{G}_{R,N}|}\right]^{T}$ and C is the penalty coefficient.

C. An Alternating Optimization Algorithm

In Section III-A and III-B, we have decomposed the original problem into two subproblems in order to find the near-optimal $\{\boldsymbol{W}_{s}\}$ and $\{\boldsymbol{\omega}_{B,k}, \boldsymbol{\omega}_{R,k}\}$, respectively. Note that the solutions of the two subproblems are only feasible solutions to (12), because we only consider one set of variables during each sub-optimization process. In this section, we design an AO algorithm to search for the global solution of (12). The procedure is detailed in Algorithm 1.

Remark 3. In each alternating process, the two subproblems can be viewed as optimizing the original problem in the direction of the descent gradient of two sets of variables, while the iterative process can be viewed as searching for a better solution from the updated results.

Algorithm 1 An Alternating Optimization Algorithm for Problem (12)

1: Set $t = 0$ and T as the alternating rounds, randomly generate a set of $\{\boldsymbol{\omega}_{B,k}^{[0]}, \boldsymbol{\omega}_{R,k}^{[0]}\}$.

2: **while** $t \leq T$ **do**

3:     Update $\left(\boldsymbol{\Lambda}_{R,n,i}^{+}\right)^{[t]} \left(\boldsymbol{\Lambda}_{R,n,i}^{-}\right)^{[t]}$ according to (23), (26) and (30).

4:     Set $k = 0$ and randomly generate an initial point $\boldsymbol{z}_0$.

5:     **repeat**

6:         Calculate:
$$\hat{\boldsymbol{v}}^{[t]} = \arg\min \rho_R + C \left\| \boldsymbol{\epsilon} \right\|$$
$$\text{s.t.} \quad \text{(33a), (33b) and (33c).}$$

7:         Update $\boldsymbol{z}_{k+1} = \hat{\boldsymbol{v}}^{[t]}$.

8:         Update $k = k + 1$.

9:     **until** convergence

10:    Update $\hat{\boldsymbol{W}}_s^{[t]}$ according to (17).

11:    Update $\boldsymbol{g}_{n,i}^{[t]}$ and $\left(\tilde{\sigma}_{R,n,i}^2\right)^{[t]}$ according to (36).

12:    Update $\left(\boldsymbol{\Gamma}_{B,m,i}^{+}\right)^{[t]}$, $\left(\boldsymbol{\Gamma}_{B,m,i}^{-}\right)^{[t]}$, $\left(\boldsymbol{\Gamma}_{R,n,i}^{+}\right)^{[t]}$ and $\left(\boldsymbol{\Gamma}_{R,n,i}^{-}\right)^{[t]}$ according to (43).

13:    Set $k = 0$ and randomly generate an initial point $\boldsymbol{z}_0$.

14:    **repeat**

15:       Calculate:
$$\hat{\boldsymbol{\omega}}^{[t]} = \arg\min \rho_B + C \left\| \boldsymbol{\epsilon} \right\|$$
$$\text{s.t.} \quad \text{(46a), (46b) and (46c).}$$

16:       Update $\boldsymbol{z}_{k+1} = \hat{\boldsymbol{\omega}}^{[t]}$.

17:       Update $k = k + 1$.

18:    **until** convergence

19:    Update $\{\hat{\boldsymbol{\omega}}_{B,k}^{[t]}, \hat{\boldsymbol{\omega}}_{R,k}^{[t]}\}$.

20:    Calculate $P_{\text{total}}^{[t]}$ according to (11).

21:    Update $\boldsymbol{\omega}_{B,k}^{[t+1]} = \hat{\boldsymbol{\omega}}_{B,k}^{[t]}$, $\boldsymbol{\omega}_{R,k}^{[t+1]} = \hat{\boldsymbol{\omega}}_{R,k}^{[t]}$.

22:    Update $t = t + 1$.

23: **end while**

Given that the constraints imposed on the RN-assisted users are considered in (35), we can guarantee that the solutions obtained at each alternate process are feasible. However, we shall clarify that sometimes the AO procedure of Algorithm 1 is not guaranteed to converge. Since the subproblems we obtained are both non-convex, only near-optimal solutions are obtained with the aid of the FPP-SCA approach. Furthermore, the AO algorithm cannot find the globally optimal solution. Fortunately, given that the optimization objective function of the original problem is convex, the AO algorithm can succeed in finding a good enough solution to problem (12), and this is numerically shown in our simulation results.

Remark 4. Here, we provide the complexity analysis of our proposed algorithm. According to [38], the worst-case computational complexities of solving the problem in (33) and (46) are $\mathcal{O}\big(\left(SN_RN+1\right)^{3.5}\big)$ and $\mathcal{O}\big(\left((N_B+1)(M+N)\right)^{3.5}\big)$, respectively. Hence, the worst-case computational complexity of an alternating process is $\mathcal{O}\left(\left(SN_RN+1\right)^{3.5}K_1+\left((N_B+1)(M+N)\right)^{3.5}K_2\right)$, where K_1 and K_2 represent the number of iterations of the FPP-SCA approach for (33) and (46), respectively.

IV. A DISTRIBUTED LOW-COMPLEXITY ALGORITHM RELYING ON ZERO-FORCING PRECODING

The algorithm proposed in Section III-C is characterized by high computational complexity, and may not be practically feasible if the number of vessel users is large. Hence in this section, we aim for designing a low-complexity algorithm having a closed-form solution relying on zero-forcing (ZF) precoding at the RNs and at BSA.

A. Relaying Vector Design for the RNs

From (27), we can see that the signal received at RNs is first combined and then transmitted to the RN-served users based on the relaying vector $\boldsymbol{v}$. The strength of the desired signal and of the interferences can be modeled as $\left|\tilde{\boldsymbol{f}}_{n,n,i}^H\boldsymbol{v}\right|^2$ and $\sum_{k=1}^M\left|\hat{\boldsymbol{f}}_{k,n,i}^H\boldsymbol{v}\right|^2+\sum_{k=1,k\neq n}^N\left|\tilde{\boldsymbol{f}}_{k,n,i}^H\boldsymbol{v}\right|^2$, respectively. Based on ZF precoding, the design of $\boldsymbol{v}^{\mathsf{ZF}}$ should satisfy the following conditions:

$$\begin{cases} \hat{\boldsymbol{f}}_{k,n,i}^H\boldsymbol{v}^{\mathsf{ZF}}=0, k=1,2,...,M, \\ \tilde{\boldsymbol{f}}_{k,n,i}^H\boldsymbol{v}^{\mathsf{ZF}}=0, k=1,2,...,n-1,n+1,...,N. \end{cases} \tag{47}$$

Upon defining $\boldsymbol{F}=\left[\hat{\boldsymbol{f}}_{1,1,1},...,\hat{\boldsymbol{f}}_{M,N,\left|\mathcal{G}_{B,M}\right|},\tilde{\boldsymbol{f}}_{1,1,1},...,\tilde{\boldsymbol{f}}_{N,N,\left|\mathcal{G}_{R,N}\right|}\right]$, we can obtain:

$$\boldsymbol{V}^{\mathsf{ZF}}=\boldsymbol{F}\big(\boldsymbol{F}^H\boldsymbol{F}\big)^{-1}, \tag{48}$$

where we have $\boldsymbol{V}^{\mathsf{ZF}}=\left[\hat{\boldsymbol{v}}_{1,1,1},...,\hat{\boldsymbol{v}}_{M,N,\left|\mathcal{G}_{B,M}\right|},\tilde{\boldsymbol{v}}_{1,1,1},...,\tilde{\boldsymbol{v}}_{N,N,\left|\mathcal{G}_{R,N}\right|}\right]$. In order to meet the conditions in (47), $\boldsymbol{v}^{\mathsf{ZF}}$ can be designed in the form of:

$$\boldsymbol{v}^{\mathsf{ZF}}=\sum_{n=1}^N\sum_{i=1}^{\left|\mathcal{G}_{R,n}\right|}\tilde{\boldsymbol{v}}_{n,n,i}. \tag{49}$$

Furthermore, $\bar{\boldsymbol{v}} \triangleq \boldsymbol{v}^{\mathsf{ZF}}/\|\boldsymbol{v}^{\mathsf{ZF}}\|$ is normalized in order to have $\boldsymbol{v} = \sqrt{p_R}\bar{\boldsymbol{v}}$. Then, (27) can be reduced to the power minimization problem of:

$$\min_{p_R} \quad p_R \bar{\boldsymbol{v}}^H \boldsymbol{Q} \bar{\boldsymbol{v}} \tag{50}$$

$$\text{s.t.} \quad \frac{p_R \left| \tilde{\boldsymbol{f}}_{n,n,i}^H \bar{\boldsymbol{v}} \right|^2}{p_R \|\boldsymbol{G}_{n,i}\bar{\boldsymbol{v}}\|^2 + \sigma_{R,n,i}^2} \geq \gamma_{R,n}, \forall n, i \in \mathcal{G}_{R,n}. \tag{50a}$$

From the constraints in (50a), we can arrive at:

$$p_R = \max_{n,i} \frac{\gamma_{R,n}\sigma_{R,n,i}^2}{\left| \tilde{\boldsymbol{f}}_{n,n,i}^H \bar{\boldsymbol{v}} \right|^2 - \gamma_{R,n}\|\boldsymbol{G}_{n,i}\bar{\boldsymbol{v}}\|^2}. \tag{51}$$

B. Beamforming Vector Optimization for BSA

In the light of ZF precoding, $\boldsymbol{\omega}_{B,k}^{\mathsf{ZF}}$ and $\boldsymbol{\omega}_{R,k}^{\mathsf{ZF}}$ should be chosen for ensuring that there is no interference between the multicast groups. The channel matrix between BSA and all the users can be formulated as:

$$\boldsymbol{H} = \left[\boldsymbol{h}_{1,1}, ..., \boldsymbol{h}_{M,|\mathcal{G}_{B,M}|}, \boldsymbol{g}_{1,1}, ..., \boldsymbol{g}_{N,|\mathcal{G}_{R,N}|} \right]. \tag{52}$$

Then, let us calculate:

$$\boldsymbol{\Omega}^{\mathsf{ZF}} = \boldsymbol{H}\big(\boldsymbol{H}^H \boldsymbol{H}\big)^{-1}, \tag{53}$$

where we have $\boldsymbol{\Omega}^{\mathsf{ZF}} = \left[\boldsymbol{\omega}_{B,1,1}, ..., \boldsymbol{\omega}_{B,M,|\mathcal{G}_{B,M}|}, \boldsymbol{\omega}_{R,1,1}, ..., \boldsymbol{\omega}_{R,N,|\mathcal{G}_{R,N}|} \right]$. For the sake of ensuring that there is no interference between different groups, we design $\boldsymbol{\omega}_{B,k}^{\mathsf{ZF}}$ and $\boldsymbol{\omega}_{R,k}^{\mathsf{ZF}}$ as:

$$\begin{cases} \boldsymbol{\omega}_{B,k}^{\mathsf{ZF}} = \sum_{i=1}^{|\mathcal{G}_{B,k}|} \boldsymbol{\omega}_{B,k,i}, \\ \boldsymbol{\omega}_{R,k}^{\mathsf{ZF}} = \sum_{i=1}^{|\mathcal{G}_{R,k}|} \boldsymbol{\omega}_{R,k,i}. \end{cases} \tag{54}$$

Let us now define $\bar{\boldsymbol{\omega}}_{B,k} \triangleq \boldsymbol{\omega}_{B,k}^{\mathsf{ZF}}/\|\boldsymbol{\omega}_{B,k}^{\mathsf{ZF}}\|$ and $\bar{\boldsymbol{\omega}}_{R,k} \triangleq \boldsymbol{\omega}_{R,k}^{\mathsf{ZF}}/\|\boldsymbol{\omega}_{R,k}^{\mathsf{ZF}}\|$. Then we have $\boldsymbol{\omega}_{B,k} = \sqrt{p_{B,k}}\bar{\boldsymbol{\omega}}_{B,k}$ and $\boldsymbol{\omega}_{R,k} = \sqrt{p_{R,k}}\bar{\boldsymbol{\omega}}_{R,k}$, respectively. As a result, the optimization objective function

in (37) can be rewritten as:

$$P_{\text{total}}^{[2]} = \sum_{k=1}^{M} p_{B,k} + \sum_{k=1}^{N} p_{R,k} + \sum_{s=1}^{S}\sum_{k=1}^{M} p_{B,k} \left\| \hat{\boldsymbol{W}}_s \boldsymbol{H}_s^H \bar{\boldsymbol{\omega}}_{B,k} \right\|^2 + \sum_{s=1}^{S}\sum_{k=1}^{N} p_{R,k} \left\| \hat{\boldsymbol{W}}_s \boldsymbol{H}_s^H \bar{\boldsymbol{\omega}}_{R,k} \right\|^2 . \tag{55}$$

Hence, (37) can be transformed into a power minimization problem, which is given by:

$$\min_{\{p_{B,k}, p_{R,k}\}} \quad P_{\text{total}}^{[2]} \tag{56}$$

$$\text{s.t.} \quad \frac{p_{B,m} \left| \boldsymbol{h}_{m,i}^H \bar{\boldsymbol{\omega}}_{B,m} \right|^2}{\sigma_{B,m,i}^2} \geq \gamma_{B,m}, \forall m, i \in \mathcal{G}_{B,m}, \tag{56a}$$

$$\frac{p_{R,n} \left| \boldsymbol{g}_{n,i}^H \bar{\boldsymbol{\omega}}_{R,n} \right|^2}{\tilde{\sigma}_{R,n,i}^2} \geq \gamma_{R,n}, \forall n, i \in \mathcal{G}_{R,n}, \tag{56b}$$

and the minimum power can be determined by:

$$\begin{cases} p_{B,m} = \max_i \dfrac{\gamma_{B,m}\sigma_{B,m,i}^2}{\left| \boldsymbol{h}_{m,i}^H \bar{\boldsymbol{\omega}}_{B,m} \right|^2}, \forall m, \\[4mm] p_{R,n} = \max_i \dfrac{\gamma_{R,n}\tilde{\sigma}_{R,n,i}^2}{\left| \boldsymbol{g}_{n,i}^H \bar{\boldsymbol{\omega}}_{R,n} \right|^2}, \forall n. \end{cases} \tag{57}$$

V. SIMULATION RESULTS

In this section, numerical results are provided for evaluating the performance of our proposed algorithm in the context of offshore areas. The communication distances of the first hop and second hop are set to be 10 km, and the path loss exponent is set to 3. The system operates at a carrier frequency of 1.9 GHz and the noise level is set to be -30 dBW. The K-factor of the Rician fading channel is set to be 12.7 dB while the means and variance of the Rayleigh fading channel are 0 and 4, respectively [29]. Moreover, high gain antennas are assumed to mitigate the attenuation, and the transmit antenna gains of the BSA and of the RNs are set to 40 and 35 dBi, respectively. We assume that there are $M = 4$ BS-aided groups and $N = 4$ RN-assisted groups. We use different SINR targets to model the circumstances of different user densities and the SINR targets for all groups are assumed to be the same for simplicity.

Fig. 3 shows the convergence performance of the FPP-SCA algorithm for the BSA beamforming vectors' optimization problem, where we assume that there are $S = 4$ RNs and each RN is equipped with $N_R = 8$ antennas. Moreover, we assume that each RN serves one group and
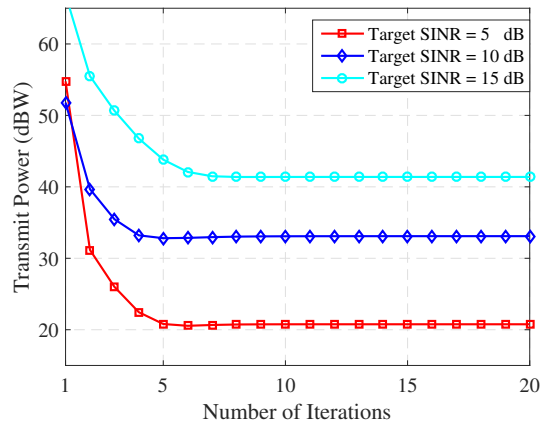
Fig. 3. The convergence performance of FPP-SCA algorithm for the S-BS's beamforming vector optimization problem with $(S, N_R) = (4, 8)$.
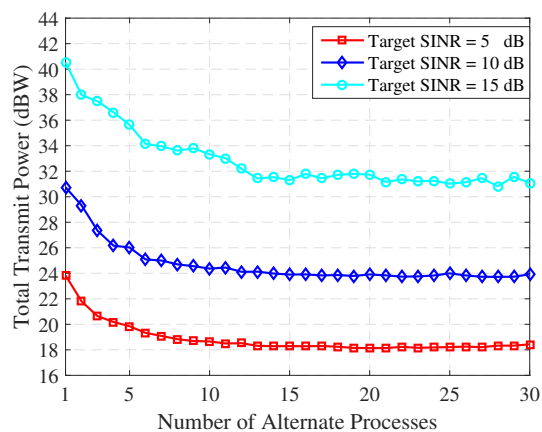
Fig. 4. The convergence performance of Algorithm 1 with $(S, N_B, N_R) = (4, 16, 8)$.

each RN-assisted group contains two single-antenna users. The processing matrices $\{\hat{\boldsymbol{W}}_s\}$ are obtained by randomly-generated $\{\boldsymbol{\omega}_{B,k}, \boldsymbol{\omega}_{R,k}\}$ values. The penalty coefficient is set to $C = 10^6$. As shown in Fig. 3, the FPP-SCA algorithm converges in terms of 5 or 6 iterations. Furthermore, as the penalty coefficient is set to a large value, relying on the FPP-SCA algorithm, the slack variable ϵ approaches zero, which yields a feasible solution to (28).

Fig. 4 portrays the convergence performance of our proposed AO algorithm, i.e. Algorithm 1, for joint beamforming optimization and relay design. Here, we assume that BSA is equipped with $N_B = 16$ downlink transmit antennas and each BS-aided group supports two single-antenna users, while the parameters with respect to the RNs and RN-assisted groups remain unchanged. The result is averaged over 50 channel realizations. It can be observed that, although the AO
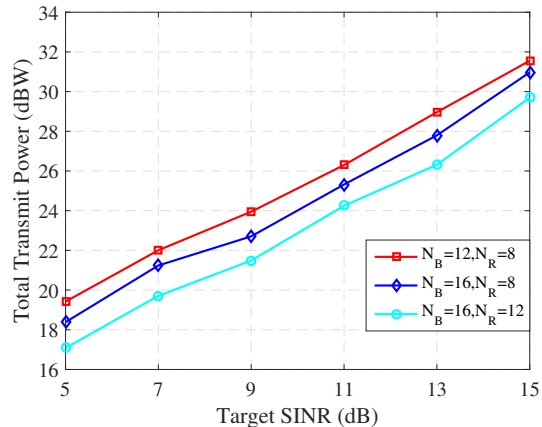
Fig. 5. The system's total transmit power versus the target SINR parameterized by different number of antennas of the S-BS and RNs with $S = 4$.
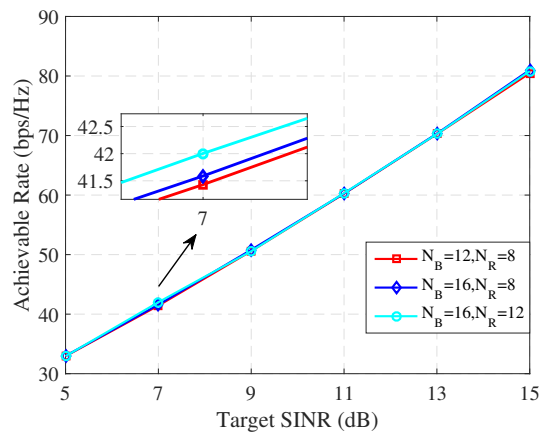
Fig. 6. The system's achievable rate versus the target SINR parameterized by different number of antennas of the S-BS and RNs with $S = 4$.

algorithm is not strictly convergent, it approached the convergent solution of (12), where the number of alternate processes is about 15 at a low target SINR. Moreover, the number of alternate processes required for approaching convergence increases upon increasing the target SINR. This is because a high target SINR results in the non-convexity of (33) and (46), which may lead to degraded solutions.

Fig. 5 and Fig. 6 evaluate the system's performance versus the target SINR parameterized by different number of antennas at BSA and at the RNs, where we assume that there are $S = 4$ RNs and each RN-assisted group contains two single-antenna users. Specifically, the system's

achievable rate is calculated by:

$$R_{\text{total}} = \sum_{m=1}^{M} \sum_{i=1}^{|\mathcal{G}_{B,m}|} \log_2 \left(1 + \text{SINR}_{B,m,i}\right) + \sum_{n=1}^{N} \sum_{i=1}^{|\mathcal{G}_{R,n}|} \log_2 \left(1 + \text{SINR}_{R,n,i}\right). \tag{58}$$

As shown in Fig. 5 and in Fig. 6, an increased transmit power is required for satisfying high target SINRs. Additionally, increasing the number of BSA antennas and RN antennas is beneficial in terms of reducing the power consumption, which is a benefit of their higher spatial diversity gain. Fig. 6 demonstrates that the system's achievable rate is insensitive to the number of antennas used, which implies that the solution obtained from Algorithm 1 approaches the boundary of the SINR constraints.

In Fig. 7 and Fig. 8, we evaluate the influence of both the group size as well as of the number of relay nodes on the system's total transmit power. In Fig. 7, we assume that there are $S = 4$ RNs. As shown in Fig. 7, more power is required for satisfying the SINR constraints of more users. Moreover, upon increasing the group size, the benefit of a large number of antennas becomes obvious. Specifically, when the number of antennas of BSA and of the RNs increases from $(12, 8)$ to $(16, 12)$, the system's total transmit power is reduced by 2.7 dBW in the context of the group size of 1, whilst by as much as 9 dBW, when the group size is 5. In Fig. 8 we assume that $N_B = 16, N_R = 8$ and the group size is set to 2. We assume that each RN mainly serves one group when $S = 4$, two groups when $S = 3$ and three groups when $S = 2$. We can conclude that the system's total transmit power consumption is reduced upon increasing the number of relay nodes. That is because increasing the number of relay nodes offloads the average number of vessel users served by one RN, which is conducive to strengthening the desired signals and reducing the interferences.

Finally, the performance of the system's total transmit power in terms of different optimization schemes is shown in Fig. 9, where we set $S = 4, N_B = 16, N_R = 8$ and the group size is 2. To elaborate, the "optimal scheme" is the method proposed in Algorithm 1, the "ZF scheme" is the algorithm described in Section IV, and the "greedy scheme" is a modified distributed algorithm relying on Algorithm 1, where the RNs and BSA use relay matrices and beamforming vectors designed separately without alternate processes. It can be seen from Fig. 9 that the ZF scheme requires 20+ dBW higher transmit power than the optimal scheme. In the context of the sparse distribution of vessel users, the ZF scheme may result in low energy efficiency, although it has
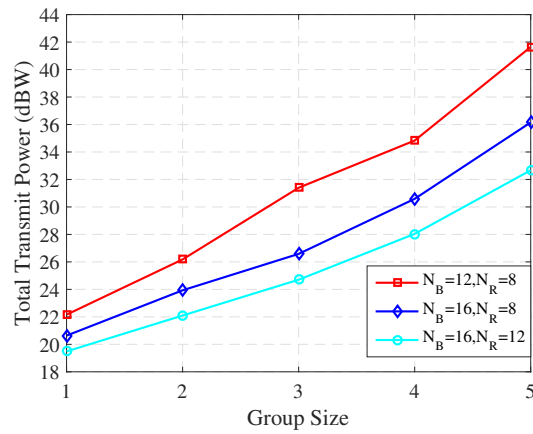
Fig. 7. The system's total transmit power versus the group size parameterized by different number of antennas of the S-BS and RNs with $S = 4$.
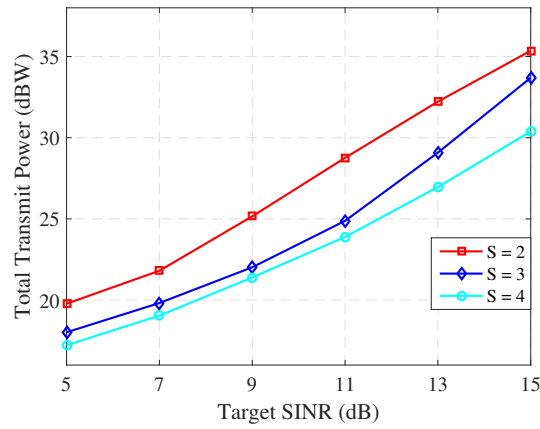
Fig. 8. The system's total transmit power versus the target SINR parameterized by different number of relay nodes with $(N_B, N_R) = (16, 8)$.
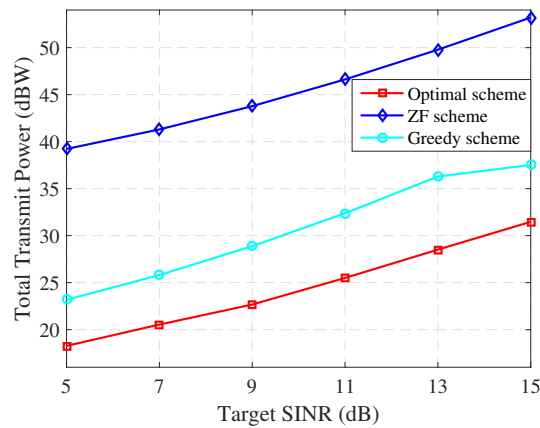
Fig. 9. The system's total transmit power in terms of different optimization schemes with $(S, N_B, N_R) = (4, 16, 8)$.

a high achievable rate. By contrast, the greedy scheme outperforms the ZF scheme. However, in comparison to the optimal scheme, it still has a 5 dBW transmit power consumption gap.

VI. CONCLUSIONS

In this paper, we investigated a multicast problem in the context of a maritime twice-hop relaying network. The SINR-guaranteed power minimization problem was formulated for jointly optimizing the beamforming and the relaying scheme. We divided the primal non-convex optimization problem into a pair of subproblems and solved them relying on the FPP-SCA approach. Furthermore, an AO algorithm as well as a low-complexity solution was presented. The numerical results showed that our algorithm is an energy-efficient solution, which is eminently suitable for challenging maritime scenarios.

APPENDIX A
PROOF OF THEOREM 1

The problem in (16) indicates that the optimal $\boldsymbol{W}_s$ should maximize the desired signal power in the numerator of (10), while minimizing the interferences, i.e. the first three terms of the denominator of (10), as well as the total transmit power. Let:

$$\boldsymbol{G}_s = \left[\boldsymbol{g}_{s,1,1}, ..., \boldsymbol{g}_{s,1,|\mathcal{G}_{R,1}|}, ..., \boldsymbol{g}_{s,N,1}, ..., \boldsymbol{g}_{s,N,|\mathcal{G}_{R,N}|}\right] \in \mathbb{C}^{N_R \times N_{RU}}, \quad (59)$$

where N_{RU} denotes the total number of RN-assisted users. Normally, we have $N_{RU} \geq N_R$. In this case, $\boldsymbol{W}_s$ can be decomposed into:

$$\begin{aligned}
\boldsymbol{W}_s &= \boldsymbol{G}_s \left[\boldsymbol{A}, \boldsymbol{B}\right] \left[\boldsymbol{R}_s, \boldsymbol{R}_s^{\perp}\right]^H \\
&= \boldsymbol{G}_s \boldsymbol{A} \boldsymbol{R}_s^H + \boldsymbol{G}_s \boldsymbol{B} \left(\boldsymbol{R}_s^{\perp}\right)^H,
\end{aligned} \quad (60)$$

where $\boldsymbol{A} \in \mathbb{C}^{N_{RU} \times N}$ and $\boldsymbol{B} \in \mathbb{C}^{N_{RU} \times (N_R - N)}$ are parameter matrices. Upon substituting (60) into (15) and (10), we have:

$$\begin{aligned}
P_{\text{total}}^{[1]} =& \sum_{s=1}^{S} \sum_{k=1}^{M} \left\| \left(\boldsymbol{G}_s \boldsymbol{A} \boldsymbol{R}_s^H + \boldsymbol{G}_s \boldsymbol{B} \left(\boldsymbol{R}_s^{\perp}\right)^H\right) \boldsymbol{H}_s^H \boldsymbol{\omega}_{B,k} \right\|^2 + \sum_{s=1}^{S} \sum_{k=1}^{N} \left\| \boldsymbol{G}_s \boldsymbol{A} \boldsymbol{R}_s^H \boldsymbol{r}_{s,k} \right\|^2 \\
&+ \sum_{s=1}^{S} \sigma_s^2 \left\| \boldsymbol{G}_s \boldsymbol{A} \boldsymbol{R}_s^H + \boldsymbol{G}_s \boldsymbol{B} \left(\boldsymbol{R}_s^{\perp}\right)^H \right\|^2,
\end{aligned} \quad (61)$$

and

$$\text{Numerator}\{\text{SINR}_{R,n,i}\} = \left| \sum_{s=1}^{S} \boldsymbol{g}_{s,n,i}^{H} \boldsymbol{G}_s \boldsymbol{A} \boldsymbol{R}_s^{H} \boldsymbol{r}_{s,n} \right|^2, \tag{62}$$

and

$$
\begin{aligned}
\text{Denominator}\{\text{SINR}_{R,n,i}\} = &\sum_{k=1}^{M} \left| \sum_{s=1}^{S} \boldsymbol{g}_{s,n,i}^{H} \left(\boldsymbol{G}_s \boldsymbol{A} \boldsymbol{R}_s^{H} + \boldsymbol{G}_s \boldsymbol{B} \left(\boldsymbol{R}_s^{\perp} \right)^{H} \right) \boldsymbol{H}_s^{H} \boldsymbol{\omega}_{B,k} \right|^2 \\
&+ \sum_{k=1,k\neq n}^{N} \left| \sum_{s=1}^{S} \boldsymbol{g}_{s,n,i}^{H} \boldsymbol{G}_s \boldsymbol{A} \boldsymbol{R}_s^{H} \boldsymbol{r}_{s,k} \right|^2 \\
&+ \sum_{s=1}^{S} \sigma_s^2 \left\| \boldsymbol{g}_{s,n,i}^{H} \left(\boldsymbol{G}_s \boldsymbol{A} \boldsymbol{R}_s^{H} + \boldsymbol{G}_s \boldsymbol{B} \left(\boldsymbol{R}_s^{\perp} \right)^{H} \right) \right\|^2 + \sigma_{R,n,i}^2.
\end{aligned} \tag{63}
$$

We can see that $\boldsymbol{B}$ has no effect on the strength of the desired signal. Furthermore, setting $\boldsymbol{B} = \boldsymbol{0}$ is capable of reducing both the interferences and the transmit power consumption. Therefore, we have:

$$\boldsymbol{W}_s = \boldsymbol{G}_s \boldsymbol{A} \boldsymbol{R}_s^{H} = \boldsymbol{V}_s \boldsymbol{R}_s^{H}. \tag{64}$$

REFERENCES

[1] D. Palma, "Enabling the maritime Internet of Things: CoAP and 6LoWPAN performance over VHF links," *IEEE Internet of Things Journal*, vol. 5, no. 6, pp. 5205–5212, Sep. 2018.

[2] T. Yang, Z. Zheng, H. Liang, R. Deng, N. Cheng, and X. Shen, "Green energy and content-aware data transmissions in maritime wireless communication networks," *IEEE Transactions on Intelligent Transportation Systems*, vol. 16, no. 2, pp. 751–762, Sep. 2015.

[3] C. Liu, W. Feng, T. Wei, and N. Ge, "Fairness-oriented hybrid precoding for massive mimo maritime downlink systems with large-scale CSIT," *China Communications*, vol. 15, no. 1, pp. 52–61, Feb. 2018.

[4] D. Kidston and T. Kunz, "Challenges and opportunities in managing maritime networks," *IEEE Communications Magazine*, vol. 46, no. 10, pp. 162–168, Oct. 2008.

[5] J. G. Puente, "The emergence of commercial digital satellite communications," *IEEE Communications Magazine*, vol. 48, no. 7, pp. 16–20, Aug. 2010.

[6] H. Boiardt and C. Rodriguez, "Low earth orbit nanosatellite communications using Iridium's network," *IEEE Aerospace and Electronic Systems Magazine*, vol. 25, no. 9, pp. 35–39, Sep. 2010.

[7] Y. Yang, H. Hu, J. Xu, and G. Mao, "Relay technologies for WiMAX and LTE-advanced mobile systems," *IEEE Communications Magazine*, vol. 47, no. 10, pp. 100–105, Oct. 2009.

[8] M.-T. Zhou, V. D. Hoang, H. Harada, J. S. Pathmasuntharam, H. Wang, P.-Y. Kong, C.-W. Ang, Y. Ge, and S. Wen, "Triton: High-speed maritime wireless mesh network," *IEEE Wireless Communications*, vol. 20, no. 5, pp. 134–142, Oct. 2013.

[9] T. Yang, H. Liang, N. Cheng, R. Deng, and X. Shen, "Efficient scheduling for video transmissions in maritime wireless communication networks," *IEEE Transactions on Vehicular Technology*, vol. 64, no. 9, pp. 4215–4229, Oct. 2015.

[10] R. Campos, T. Oliveira, N. Cruz, A. Matos, and J. M. Almeida, "BLUECOM+: Cost-effective broadband communications at remote ocean areas," in *IEEE OCEANS*, Shanghai, China, Jun. 2016, pp. 1–6.

[11] L. Mroueh, A. Kessab, P. Martins, S. Hethuin, and E. Vivier, "Radio resource dimensioning in a centralized ad-hoc maritime MIMO LTE network," in *IEEE 36th Sarnoff Symposium*, Newark, NJ, Sep. 2015, pp. 128–133.

[12] H. Wang, P. Pan, L. Shen, and Z. Zhao, "On the pair-wise error probability of a multi-cell mimo uplink system with pilot contamination," *IEEE Transactions on Wireless Communications*, vol. 13, no. 10, pp. 5797–5811, Jul. 2014.

[13] P. Pan, H. Wang, Z. Zhao, and W. Zhang, "How many antenna arrays are dense enough in massive mimo systems," *IEEE Transactions on Vehicular Technology*, vol. 67, no. 4, pp. 3042–3053, Nov. 2017.

[14] T. Wei, W. Feng, N. Ge, and J. Lu, "Optimized time-shifted pilots for maritime massive MIMO communication systems," in *IEEE Wireless and Optical Communication Conference (WOCC)*, Newark, NJ, Apr. 2017, pp. 1–5.

[15] T. Yang, Z. Cui, R. Wang, J. Zhao, Z. Su, and R. Deng, "A multi-vessels cooperation scheduling for networked maritime fog-ran architecture leveraging SDN," *Peer-to-Peer Networking and Applications*, vol. 11, no. 4, pp. 1–13, Jul. 2018.

[16] Y. Xu, "Quality of service provisions for maritime communications based on cellular networks," *IEEE Access*, vol. 5, pp. 23 881–23 890, Oct. 2017.

[17] N. D. Sidiropoulos, T. N. Davidson, and Z.-Q. Luo, "Transmit beamforming for physical-layer multicasting," *IEEE Transactions on Signal Processing*, vol. 54, no. 6, pp. 2239–2251, Jun. 2006.

[18] E. Karipidis, N. D. Sidiropoulos, and Z.-Q. Luo, "Quality of service and max-min fair transmit beamforming to multiple cochannel multicast groups," *IEEE Transactions on Signal Processing*, vol. 56, no. 3, pp. 1268–1279, Mar. 2008.

[19] Z. Xiang, M. Tao, and X. Wang, "Coordinated multicast beamforming in multicell networks," *IEEE Transactions on Wireless Communications*, vol. 12, no. 1, pp. 12–21, Jan. 2013.

[20] H. Zhang, C. Jiang, L. Kuang, Y. Qian, and S. Guo, "Cooperative QoS beamforming for multicast transmission in terrestrial-satellite networks," in *IEEE Global Communications Conference (GLOBECOM) 2017*, Singapore, Singapore, Dec. 2017, pp. 1–6.

[21] Z. Xiang, M. Tao, and X. Wang, "Massive MIMO multicasting in noncooperative cellular networks," *IEEE Journal on Selected Areas in Communications*, vol. 32, no. 6, pp. 1180–1193, Jun. 2014.

[22] N. Bornhorst, M. Pesavento, and A. B. Gershman, "Distributed beamforming for multi-group multicasting relay networks," *IEEE Transactions on Signal Processing*, vol. 60, no. 1, pp. 221–232, Sep. 2012.

[23] M. Dong and B. Liang, "Multicast relay beamforming through dual approach," in *IEEE 5th International Workshop on Computational Advances in Multi-Sensor Adaptive Processing (CAMSAP)*, St. Martin, France, Jan. 2013, pp. 492–495.

[24] S. Li, W. Xu, K. Yang, K. Niu, and J. Lin, "Distributed cooperative multicast in cognitive multi-relay multi-antenna systems," *IEEE Signal Processing Letters*, vol. 22, no. 3, pp. 288–292, Sep. 2015.

[25] J. Du, M. Xiao, M. Skoglund, and M. Médard, "Wireless multicast relay networks with limited-rate source-conferencing," *IEEE Journal on Selected Areas in Communications*, vol. 31, no. 8, pp. 1390–1401, Oct. 2013.

[26] G. Zhao, W. Shi, Z. Chen, and Q. Zhang, "Autonomous relaying scheme with minimum user power consumption in

cooperative multicast communications," *IEEE Transactions on Wireless Communications*, vol. 15, no. 4, pp. 2509–2522, Dec.

[27] S. X. Wu, Q. Li, A. M.-C. So, and W.-K. Ma, "A stochastic beamformed amplify-and-forward scheme in a multigroup multicast MIMO relay network with per-antenna power constraints," *IEEE Transactions on Wireless Communications*, vol. 15, no. 7, pp. 4973–4986, Apr. 2016.

[28] Y. Zhou, H. Liu, Z. Pan, L. Tian, and J. Shi, "Cooperative multicast with location aware distributed mobile relay selection: Performance analysis and optimized design," *IEEE Transactions on Vehicular Technology*, vol. 66, no. 9, pp. 8291–8302, Mar. 2017.

[29] J. Wang, H. Zhou, Y. Li, Q. Sun, Y. Wu, S. Jin, T. Q. Quek, and C. Xu, "Wireless channel models for maritime communications," *IEEE Access*, vol. 6, pp. 68 070–68 088, Nov. 2018.

[30] S. Balkees, K. Sasidhar, and S. Rao, "A survey based analysis of propagation models over the sea," in *IEEE International Conference on Advances in Computing, Communications and Informatics (ICACCI)*, Kochi, India, Sept. 2015, pp. 69–75.

[31] M. Afshang, C. Saha, and H. S. Dhillon, "Nearest-neighbor and contact distance distributions for Thomas cluster process," *IEEE Wireless Communications Letters*, vol. 6, no. 1, pp. 130–133, Dec. 2017.

[32] M. Afshang, H. S. Dhillon, and P. H. J. Chong, "Modeling and performance analysis of clustered device-to-device networks," *IEEE Transactions on Wireless Communications*, vol. 15, no. 7, pp. 4957–4972, Apr. 2016.

[33] H. Tang, W. Chen, J. Li, and H. Wan, "Achieving global optimality for joint source and relay beamforming design in two-hop relay channels," *IEEE Transactions on Vehicular Technology*, vol. 63, no. 9, pp. 4422–4435, Mar. 2014.

[34] B. Khoshnevis, W. Yu, and R. Adve, "Grassmannian beamforming for MIMO amplify-and-forward relaying," *IEEE Journal on Selected Areas in Communications*, vol. 26, no. 8, pp. 1397–1408, Oct. 2008.

[35] S. Song and Q. Zhang, "Design collaborative systems with multiple AF-relays for asynchronous frequency-selective fading channels," *IEEE Transactions on Communications*, vol. 57, no. 9, pp. 2808–2817, Oct. 2009.

[36] X. Tang and Y. Hua, "Optimal design of non-regenerative MIMO wireless relays," *IEEE Transactions on Wireless Communications*, vol. 6, no. 4, pp. 1398–1407, Apr. 2007.

[37] W.-K. Ma, T. N. Davidson, K. M. Wong, Z.-Q. Luo, and P.-C. Ching, "Quasi-maximum-likelihood multiuser detection using semi-definite relaxation with application to synchronous CDMA," *IEEE Transactions on Signal Processing*, vol. 50, no. 4, pp. 912–922, Aug. 2002.

[38] O. Mehanna, K. Huang, B. Gopalakrishnan, A. Konar, and N. D. Sidiropoulos, "Feasible point pursuit and successive approximation of non-convex QCQPs," *IEEE Signal Processing Letters*, vol. 22, no. 7, pp. 804–808, Nov. 2015.